CONTRIBUTION OF TITIN TO THE IMPROVED EXERCISE-INDUCED CARDIAC COMPLIANCE AND THE FUNCTIONAL EFFECTS OF DETRAINING IN THE RAT MODEL OF ATHLETE'S HEART

PhD Thesis

Dalma Lucia Kellermayer, MD

Doctoral School of Theoretical and Translational Medicine

Semmelweis University

Supervisor: Tamás Radovits, MD, PhD

Official reviewers: Attila Borbély, MD, PhD
Éva Ruisanchez, MD, PhD

Head of the Complex Examination Committee:
István Karádi, MD, DSc

Members of the Complex Examination Committee:
Péter Andréka, MD, DSc
Henriette Farkas, MD, PhD

Budapest
2022

1. Introduction

Long-term exercise induces complex physiological cardiac remodelling, referred to as athlete's heart. It is characterized by left ventricular (LV) hypertrophy, increased LV mass, wall thickness and enlarged cavities. Moreover, long-term exercise improves the contractility, relaxation and mechanoenergetic status of the heart.

Additionally, athlete's heart was shown to be associated with improved left ventricular (LV) diastolic function and hence cardiac compliance. Cardiac compliance is predominantly regulated by the giant elastic protein, titin.

The main roles of titin are to determine the elastic, contractile and signaling properties of striated muscles. The I-band region of titin functions as a molecular spring and it contains the N2B unique sequence and the PEVK element. The adult cardiac muscle contains two main titin isoforms; the more compliant N2BA and the stiffer N2B titin. Elevated N2BA/N2B ratio is associated with reduced passive stiffness and improved ventricular compliance. Moreover, the PEVK and N2B elements have specific phosphorylation sites that allow for post-translational adjustment of titin-based stiffness. Reduced passive stiffness is associated with increased exercise tolerance and cardiac compliance. Previous studies revealed modified titin compliance via post-translational phosphorylation after acute and chronic exercise. Furthermore, increased N2BA titin isoform content was reported in rats using voluntary running wheel exercise method. However, no data are available on the impact of titin modifications on cardiac sarcomere structure and mechanics after long-term exercise.

On the other hand, the effects of training reduction (detraining or deconditioning) are less understood. Multiple evaluations reported regression of exercise-induced morphological alterations in athletes and in experimental animals.

Nevertheless, functional reversibility of athlete's heart has been reported in only a few experimental studies using isolated cardiomyocytes and papillary muscle studies. Furthermore, solely a few human echocardiographic and cardiac magnetic resonant evaluations using traditional load-dependent parameters suggest the possible functional reversibility of athlete's heart. However, the effects of detraining on the functional performance of an intact heart still has not been reported. Left ventricular (LV) pressure–volume (P–V) analysis provides the possibility of *in vivo* characterization of cardiac function and mechanics in human studies and experimental animals. The use of this sensitive method might answer the essential question whether the improved cardiac performance would still persist or an impaired function would develop in the heart of highly-trained athletes after detraining. However, because of the invasive nature of this method, animal models are required to investigate the essential questions of sports cardiology.

2. Objectives

The purpose and aims of the present study were:

1) Evaluation of titin's role in the improved cardiac compliance of exercise-induced left ventricular hypertrophy.
   i) Induction of athlete's heart by a 12-week-long swim training protocol in a rat model. Assessment of LV hypertrophy by echocardiography and tissue weights.
   ii) Examine total titin content, titin isoform expression and post-translational phosphorylation of titin of the left ventricle by using molecular biological methods.
   iii) Determine whether any training-induced titin modification has an impact on the sarcomere structure and elasticity of single myofibrils isolated from the left ventricle by atomic force microscopy (AFM).
2) Investigate the effects of detraining on left ventricular performance.
   i) Evaluate the morphological reversibility of exercise-induced LV hypertrophy by echocardiography, tissue weights and histology after an 8-week-long detraining period.
   ii) Provide detailed characterization of *in vivo* LV haemodynamic alterations (contractility, relaxation, stiffness, cardiac energetics) after the cessation of exercise by LV pressure-volume (P-V) analysis.

3. Methods

3.1. Animal model

All of the animal experimental procedures were approved by the Ethical Committee of Hungary for Animal Experimentation (License number: PEI/001/2374-4/2015). Young adult male Wistar rats (12-week-old, n = 28, m= 275–325 g) were randomly divided into control (Co, n = 14), exercised (Ex, n = 14), detrained control (DCo, n=8) and detrained exercise (DEx, n=8) groups. Rats of the Ex and DEx groups swam 200 min/day 5 days/week for 12 weeks to induce physiological LV hypertrophy. Co and DCo animals were habituated to water 5 min/day to eliminate the possible differences induced by the stress of water contact.

3.2. Echocardiography

Echocardiographic measurements were performed after the training (12 wk) and detraining period (20 wk) under pentobarbital sodium (60 mg/kg ip.) anesthesia. Two-dimensional and M-mode echocardiographic images of long and short (midpapillary-level) axis were recorded. LV anterior wall thickness (AWT), posterior wall thickness (PWT) in diastole (index d) and systole (index s), and LV end-diastolic (LVEDD) and end-systolic diameters (LVESD) were measured. LV mass and LV mass index was calculated according to a cubic formula: LV mass = $\{[(LVEDD + AWTd + PWTd)^3 - LVEDD^3] \times 1.04\} \times 0.8 + 0.14$. LV mass values were standardized to the animal's body weight to calculate LV mass index. To characterize LV systolic function, LV fractional shortening [FS = (LVEDD - LVESD)/LVEDD x 100] and LV ejection fraction (EF) were calculated.

3.3. Titin isoform analysis and titin phosphorylation

Titin isoform ratio (N2BA/N2B) was determined by large format 1% sodium-dodecyl-sulfate (SDS) - agarose gel electrophoresis. Relative content of total titin (TT) was normalized to myosin heavy chain (MHC). T2 (titin's proteolytic degradation product) was normalized to TT. We determined total titin phosphorylation by Pro-Q Diamond staining.

To determine the phosphorylation level of titin's PEVK at pS11878 and pS12022 phosphosites, Western blot was performed. The phosphorylation signal was normalized to anti-T12 antibody signal (detecting titin's N-terminus).

3.4. Atomic Force Microscopy (AFM) Imaging and Force Spectroscopy

Resonant-mode (AC- or non-contact mode) scanning AFM was performed under liquid with silicon nitride cantilevers to examine the sarcomere structure and elasticity of single cardiac myofibrils. We determined the sarcomere length and identified the Z-disk, I-band, A-band and M-band regions on the surface profile of each myofibril. For force spectroscopic and transverse elasticity measurements we used fast force mapping (FFM, or "jumping-mode" AFM).

3.5. Haemodynamic measurements - LV pressure-volume (P–V) analysis

LV *in vivo* P-V analysis was performed to evaluate cardiac function. The following parameters were measured by P-V analysis: mean arterial pressure (MAP) and heart rate (HR), LV end-systolic pressure (LVESP), LV end-diastolic pressure (LVEDP), the maximal slope of LV systolic pressure increment (dP/dt_{max}) and diastolic

pressure decrement (dP/dt_{min}), time constant of LV pressure decay (τ, according to the Glantz method), LV end-systolic volume (LVESV), LV end-diastolic volume (LVEDV), stroke volume (SV), cardiac output (CO), EF, stroke work (SW), and arterial elastance (Ea). CO was normalized to body weight (cardiac index [CI]). Total peripheral resistance (TPR) was calculated as: TPR = MAP/CO. Furthermore, we determined load-independent contractility indices: the slope of the LV end-systolic P–V relationship (ESPVR), the preload recruitable SW (PRSW), and the slope of dP/dt_{max} - end-diastolic volume relationship (dP/dt_{max}-EDV). Additionally, we determined the slope of end-diastolic P–V relationship (EDPVR). To characterize the mechanoenergetic status of the left ventricle, mechanical efficiency (Eff) and ventriculoarterial coupling (VAC) was calculated.

3.6. Histology

Hematoxylin–eosin (HE) and picrosirius red stained sections were performed to determine cardiomyocyte width and collagen content.

3.7. Statistical analysis

Data are presented as mean ± SEM. Statistics were calculated with GraphPad Prism (GraphPad Software, La Jolla, CA, USA). Normal distribution was tested using the Shapiro–Wilk test and unpaired Student's t-test was performed. For echocardiography, mixed ANOVA test was used, post hoc pairwise comparisons with Bonferroni correction were performed to determine differences between groups (DCo vs. DEx). p-value < 0.05 was considered to be statistically significant.

For AFM, image postprocessing and data analysis were performed by using the AFM driving software.

4. Results

4.1. Exercise-induced cardiac hypertrophy

Left ventricular wall dimensions (anterior and posterior wall thickness), LV mass and LV mass index were significantly increased in trained rats after the 12-week-long swimming period. Furthermore, the heart weight, heart weight-to-body weight ratio (HW/BW) and HW to tibia length (HW/TL) ratio increased significantly in exercised animals. These results indicate the development of cardiac hypertrophy and thus athlete's heart. Echocardiographic measurements further showed improved ejection fraction (EF) and fractional shortening (FS) in exercised rats.

4.2. Alterations in titin content and phosphorylation in athlete's heart

N2BA/N2B increased significantly in the Ex group, indicating a shift towards the more compliant titin isoform (Figure 1.). The relative expression of total titin (TT) to myosin heavy chain (MHC) and T2 to TT showed no differences in the Co and Ex groups.

Total titin phosphorylation did not differ between the Co and Ex groups. However, we detected hypophosphorylation of the PS11878 site (Figure 1.) and unaltered PS12022 phosphorylation of the PEVK element, indicating an exercise-specific phosphorylation effect.

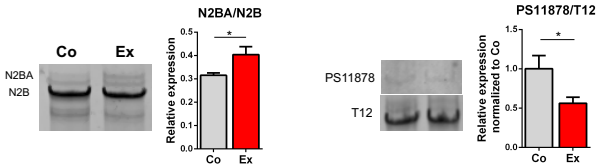

Figure 1. Increased titin isoform ratio and reduced phosphorylation of the PS11878 phosphosite was revealed in the Ex group.

4.3. Sarcomere structure and elasticity of exercised cardiac myofibrils

Atomic force microscopy measurements revealed slight differences in the sarcomeric structural dimensions of single permeabilized exercised cardiac myofibrils compared to controls.

Significantly shorter sarcomere length (SL) was measured in the Ex myofibrils. Nevertheless, the SL was in the physiological slack length range (1.7–2.2 μm) in both groups. No alterations were seen in the I-band length/SL and the A-band length/SL in the two groups. We did not find differences in the I-band/Z-disk height and the I-band/M-band height between the Co and Ex myofibrils. The Z-disk/M-band height decreased significantly in the exercised myofibrils. Overall, the Ex myofibrils displayed an irregular contour and surface profile while control myofibrils retained a more regular sarcomeric structure (Figure 2.).

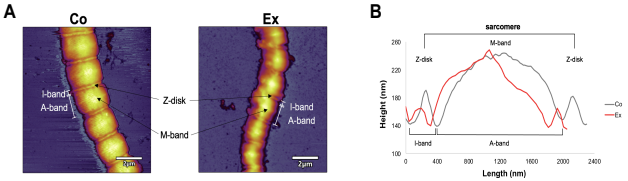

Figure 2. Topographical structure of relaxed myofibrils with AFM. A, Representative AFM images of control and exercised myofibrils. B, Representative topographical surface profile of each group. Altered topographical structure was detected in the exercised myofibrils.

The lateral stiffness (Young's modulus) was significantly decreased in the Ex myofibrils by FFM, indicating improved sarcomeric compliance (Figure 3.). Conceivably, this causes the

irregularity of the contour and surface profile of the exercised myofibrils.

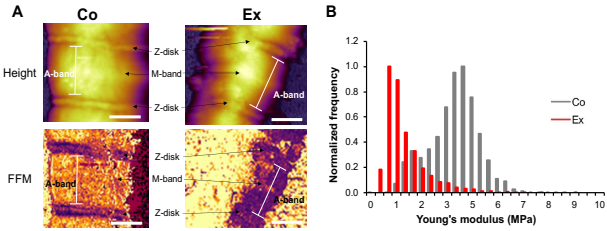

Figure 3. FFM of the sarcomeres. A, Height image and stiffness map of a Co and Ex sarcomere. B, The Young's modulus was significantly reduced in the exercised myofibrils.

4.4. Effects of detraining on cardiac morphology

The LV anterior and posterior wall thickness, LV mass and LV mass index showed complete regression after 8 weeks of detraining. Furthermore, the heart weight and heart weight-to-body weight ratio and cardiomyocyte diameters were equal in the DCo and DEx rats. The EF and FS also equalized in the control and exercised groups after deconditioning. LV collagen, determined with picrosirius red staining, was unaltered in the two groups after the detraining period.

4.5. Cardiac function after detraining

4.5.1. Baseline haemodynamic and cardiac contractility and diastolic parameters

Left ventricular pressure-volume analysis revealed similar LV pressure and dP/dt data in the DCo and DEx groups. No differences were found in the baseline haemodynamic parameters (HR, MAP, LVESP, LVEDP, LVEDV, LVESV, SV, TPR) in the DEx and DCo animals after the detraining period.

EF, CO, CI, dP/dt_{max} showed complete regression after the 8-week-long detraining period. The load-independent specific contractility indices ESPVR, PRSW and dP/dt_{max} -EDV parameters were equal after detraining (Figure 4.).

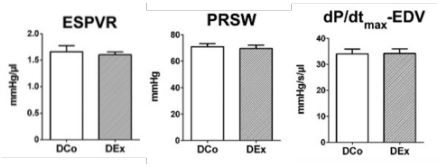

Figure 4. The load-independent contractility indices did not show any differences between the two groups after deconditioning.

The active relaxation parameters, dP/dt_{min} and τ were unaltered in the DCo and DEx animals. LVEDP and EDPVR, that describe the passive stiffness of the heart, also showed no differences in the two groups.

4.5.2. Mechanoenergetic status of the heart

The mechanoenergetic condition of the heart was comparable in the detrained rats. No differences were found in the mechanical efficiency and ventriculo-arterial coupling (VAC) of DCo and DEx animals (Figure 5.). All together, the functional (systolic, diastolic) performance and mechanoenergetic status of the athlete's heart is completely reversible after the cessation of training.

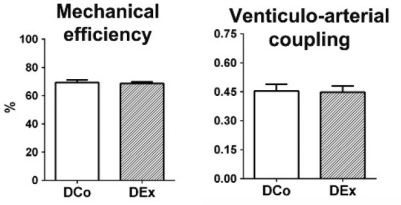

Figure 5. The mechanoenergetic status of the athlete's heart regressed completely after the 8-week-long detraining period.

5. Conclusions

We evaluated titin alterations in the cardiac muscle after long-term exercise. The significantly increased N2BA/N2B titin ratio along with the decreased phosphorylation of titin's PEVK element suggests reduced titin-based passive stiffness and a more compliant heart after chronic exercise. To our knowledge, this is the first study to reveal decreased Young's modulus in cardiac myofibrils of the athlete's heart that is associated with decreased passive stiffness and more compliant conditions. Overall, titin modifications in the athlete's heart are potential mechanisms to improve cardiac compliance and provide the best adaptation and performance to the increased circulatory demand of long-term exercise.

Additionally, we investigated the effects of detraining on the athlete's heart. We revealed complete morphological and functional regression of exercise-induced cardiac adaptation after 8 weeks of deconditioning. LV hypertrophy regressed completely after deconditioning with unaltered LV collagen content. Based on our sensitive pressure-volume analysis, we demonstrated equal data of the contractility and relaxation parameters in the detrained control and exercised rats. Furthermore, the cardiac energetics did not show any differences in the detrained animals. All together, these results indicate morphological and functional reversibility of the exercise-induced LV hypertrophy and the improved myocardial contractility and mechanoenergetic status. Moreover, to the best of our knowledge, this is the first study to report functional reversibility of athlete's heart by *in vivo* P-V haemodynamic characterization.

6. Bibliography of the candidate's publications

6.1. Publications related to the PhD thesis

Oláh A*, **Kellermayer D***, Mátyás C, Németh BT, Lux Á, Szabó L, Török M, Ruppert M, Meltzer A, Sayour AA, Benke K, Hartyánszky I, Merkely B*, Radovits T*. (2017)
Complete Reversion of Cardiac Functional Adaptation Induced by Exercise Training. Med Sci Sports Exerc, 49: 420-429.
IF: 4.291
*: equal contribution

Kellermayer D, Kiss B, Tordai H, Oláh A, Granzier HL, Merkely B, Kellermayer M*, Radovits T*. (2021)
Increased Expression of N2BA Titin Corresponds to More Compliant Myofibrils in Athlete's Heart. Int J Mol Sci, 22: 11110.
IF: 6.208
*: equal contribution

Kellermayer D, Kiss B, Mártonfalvi Z, Radovits T, Merkely B, Kellermayer M. (2020)
Az izomrugalmasság óriásfehérjéje, a titin. Magyar Sporttudományi Szemle, 3: 3-12.
IF: -

6.2. Publications not related to the PhD thesis

Radovits T, Oláh A, Lux Á, Németh BT, Hidi L, Birtalan E, **Kellermayer D**, Mátyás C, Szabó G, Merkely B. (2013)
Rat model of exercise-induced cardiac hypertrophy – hemodynamic characterization using left ventricular pressure-volume analysis. Am J Physiol Heart Circ Physiol, 305: H124-34.

IF: 4.012

Oláh A, Németh BT, Mátyás C, Horváth EM, Hidi L, Birtalan E, **Kellermayer D,** Ruppert M, Merkely G, Szabó G, Merkely B, Radovits T. (2015)
Cardiac effects of acute exhaustive exercise in a rat model. Int J Cardiol, 182: 258-66.
IF: 4.638

Kovács A, Oláh A, Lux Á, Mátyás C, Németh BT, **Kellermayer D**, Ruppert M, Török M, Szabó L, Meltzer A, Assabiny A, Birtalan E, Merkely B, Radovits T. (2015)
Strain and strain rate by speckle tracking echocardiography correlate with pressure-volume loop derived contractility indices in a rat model of athlete's heart. Am J Physiol Heart Circ Physiol, 308: H743-8.
IF: 3.324

Mátyás C, Németh BT, Oláh A, Hidi L, Birtalan E, **Kellermayer D**, Ruppert M, Korkmaz S, Kökény G, Horváth EM, Szabó G, Merkely B, Radovits T. (2015)
The soluble guanylate cyclase activator cinaciguat prevents cardiac dysfunction in a rat model of type-1 diabetes mellitus. Cardiovasc Diabetol, 14: 145.
IF: 4.534

Oláh A, Németh BT, Mátyás C, Hidi L, Lux Á, Ruppert M, **Kellermayer D**, Sayour AA, Szabó L, Török M, Meltzer A, Gellér L, Merkely B, Radovits T. (2016)

Physiological and pathological left ventricular hypertrophy of comparable degree is associated with characteristic differences of in vivo hemodynamics. Am J Physiol Heart Circ Physiol, 310: H587-97.
IF: 3.348

Németh BT, Mátyás C, Oláh A, Lux Á, Hidi L, Ruppert M, **Kellermayer D**, Kökény G, Szabó G, Merkely B, Radovits T. (2016)
Cinaciguat prevents the development of pathologic hypertrophy in a rat model of left ventricular pressure overload. Sci Rep, 6: 37166.
IF: 4.259

Mátyás C, Németh BT, Oláh A, Török M, Ruppert M, **Kellermayer D**, Barta BA, Szabó G, Kökény G, Horváth EM, Bódi B, Papp Z, Merkely B, Radovits T. (2017)
Prevention of the development of heart failure with preserved ejection fraction by the phosphodiesterase-5A inhibitor vardenafil in rats with type 2 diabetes. Eur J Heart Fail, 19: 326-336.
IF: 10.683

Kellermayer D, Smith JE 3rd, Granzier H. (2017)
Novex-3, the tiny titin of muscle. Biophys Rev, 9: 201-206.
IF: -

Oláh A, Kovács A, Lux Á, Tokodi M, Braun S, Lakatos BK, Mátyás C, **Kellermayer D**, Ruppert M, Sayour AA, Barta BA, Merkely B, Radovits T. (2019)
Characterization of the Dynamic Changes in Left Ventricular Morphology and Function Induced by Exercise Training and Detraining. Int J Cardiol, 277:178-185.
IF: 3.229

Kellermayer D, Smith JE 3rd, Granzier H. (2019)
Titin Mutations and Muscle Disease. Pflugers Arch, 471: 673-682.
IF: 3.158

Oláh A, Mátyás C, **Kellermayer D**, Ruppert M, Barta BA, Sayour AA, Török M, Koncsos G, Giricz Z, Ferdinandy P, Merkely B, Radovits T. (2019)
Sex Differences in Morphological and Functional Aspects of Exercise-Induced Cardiac Hypertrophy in a Rat Model. Front Physiol, 10: 889.
IF: 3.367

Sziklai D, Sallai J, Papp Z, **Kellermayer D**, Mártonfalvi Z, Pires RH, Kellermayer MSZ. (2022)
Nanosurgical Manipulation of Titin and Its M-Complex. Nanomaterials (Basel), 12: 178.
IF: 5.719